THE FRACTURE MECHANICS APPROACH TO UNDERSTANDING SUPPORTS IN UNDERGROUND COAL MINES

By James M. Kramer, Ph.D.,[1] George J. Karabin, P.E.,[2] and M. Terry Hoch[3]

ABSTRACT

This paper introduces the fracture mechanics approach—a unique way to predict the stability of a coal mine panel. The technique uses analytic equations to calculate the stress, strain, and yield characteristics of coal support systems. It uses fracture mechanics to model almost every type of mine support structure. Another feature is a method that incorporates field-tested knowledge into the analytical analysis. For example, this technique can model the yield characteristics of a coal seam by combining empirical pillar strength equations into the analytic analysis. It may be possible to simulate multiple-seam mining by incorporating subsidence methods into the analysis. The method is simple and quick, which makes it attractive for stress analysis software. It should be more accessible to those in the mining industry who do not have expertise in rock mechanics or numerical modeling. Although the purpose of this research is for modeling coal mines, it should be adaptable to any mine in a tabular deposit.

[1]Mining engineer.
[2]Supervisory civil engineer.
[3]Chief.
Roof Control Division, Pittsburgh Safety and Health Technology Center, Mine Safety and Health Administration, Pittsburgh, PA.

INTRODUCTION

This paper presents a new way to analyze the mechanical behavior of underground coal mine supports. Included are analytic expressions describing the stress, strain, and yielding characteristics of a coal seam. The *fracture mechanics approach* (FMA) provides the capability to model almost every type of mine structure, including pillars, yield pillars, longwall gob, chocks, cribs, posts, and hydrostatic loads. In addition, it predicts pillar stability by combining empirical pillar strength equations into the analytic analysis. This makes the procedure useful for understanding how various support structures affect the mechanical performance of a mine panel.

Although the method is not as sophisticated as numerical analysis, it offers several advantages. The analytic equation makes it is as accurate as numerical modeling, but quicker and easier to use. Because of the few equations involved, it is easy to incorporate the process into a computer spreadsheet or programmable calculator. Real-time design analysis is possible by incorporating the technique into computer code. For example, one can change a design structure (e.g., add a crib) and see instantly the resultant stress effect. The coal yielding process uses empirical pillar strength equations derived from years of field measurements. Combining these equations into the analytic analysis provides insight into pillar stability. The system presented in this paper offers a unique perspective from which to study mine panel stability.

DESIGNING SUPPORT STRUCTURES FOR COAL MINES

There are several ways to analyze the stability of a mine layout. The easiest and, in some cases, most reliable is to use pillar strength equations. These equations are developed from extensive knowledge of coal seam behavior [Mark and Iannacchione 1992]. Most are based on physical stress measurements; however, some come from numerical studies or analytic equations. All of these methods use the pillar width-to-height ratio as the controlling factor. These strength equations can be accurate; however, they assume that the coal pillar is the single means of support. It is not possible to study the effects of cribs, posts, longwall gob, chocks, etc. Also, these equations do not predict the stress distribution through the panel, nor do they predict the extent of the yield zone in the coal.

There are other, more accurate, ways to analyze stability. Numerical modeling, if used properly, can be very accurate. It can predict the stress distribution throughout the entire mine environment, including the coal seam, surrounding strata, slips, faults, and all types of supports. However, this method is time-consuming and requires a certain amount of technical skill. For example, using finite elements, it would take a skilled engineer a day or more to analyze the yield zone in a coal pillar based on data derived from field measurements.

This paper discusses a simple, quick, and accurate solution for predicting the stress distribution in coal pillars and other structures. It uses a combination of fracture mechanics and empirically derived techniques to predict the extent of the yield zone in a coal pillar. It can model nearly every structure used for mine support. Numerical modeling will validate the accuracy of the technique.

THE FRACTURE MECHANICS APPROACH

Understanding the FMA requires visualizing a coal seam as an extremely thin layer in the stratum of the Earth. A tunnel or opening in the coal would appear as a thin crack in an infinite mass.[4] It should then make sense that it is possible to use the mechanics of cracks to analyze the stresses surrounding openings in coal seams.

Visualizing a mine opening as a crack is not new; others applied it to their research [Barenblatt 1962; Hacket 1959; Crouch and Fairhurst 1973; Berry 1960, 1963]. However, this paper describes a way to use the fracture mechanics directly to predict pillar stress. Combined with a superpositioning technique, it is possible to obtain the complete stress distribution throughout the mine panel. A yielding technique completes the analysis by offering realistic characteristics to the coal pillars.

Westergaard's equation is fundamental to fracture mechanics theory and is also the basic equation for the FMA [Westergaard 1939]. The stress distribution at the crack tip is identical to the distribution adjacent to a mine opening. Westergaard describes the stress at the tip of a crack as

$$F_y(x) = \frac{Fx}{\sqrt{x^2 - a^2}}, \qquad (1)$$

[4] In this paper, the term “crack” infers a mine opening and vice versa. Therefore, crack-tip stress is the same as rib or pillar stress.

where $F_y(x)$ ' stress distribution adjacent to a crack tip,

a ' 1/2 the crack width,

F ' in situ stress,

and x ' distance from the center of the crack.

This equation implies that the only parameters needed to predict elastic rib stress are the entry width and the in situ stress (figure 1). Westergaard derived equation 1 by assuming that the stress field acting on the crack is located at an infinite distance from the crack surface. Another assumption is that the crack width must align with the planes of this stress field. In general, these conditions are similar to a mine environment. The Westergaard equation will accurately predict the stress distribution into the coal seam provided that the analysis remains within the elastic range.

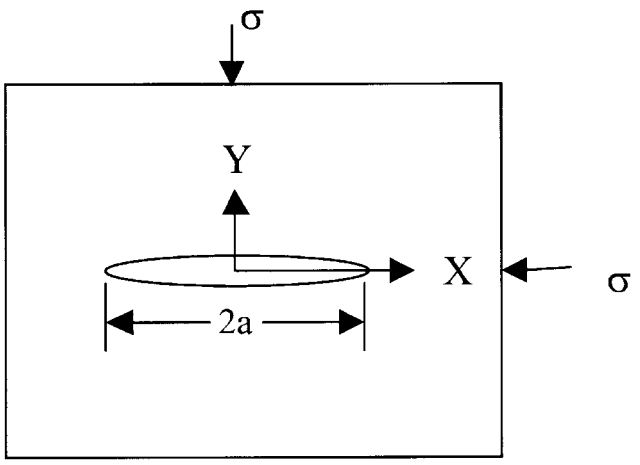

Figure 1.—Crack of width 2a subjected to a uniform biaxial stress field.

NUMERICAL METHODS VALIDATE THE WESTERGAARD EQUATION FOR MINE ANALYSIS

Westergaard developed his stress function by making the following assumptions: the crack has a thickness of zero; it is contained in an infinite, homogeneous plate; and the plate is subjected to a uniform biaxial stress field. These conditions match fairly the conditions encountered in a coal mine opening. There are differences, however. A mine opening has an actual thickness. The structural properties of the coal differ from those of the surrounding rock mass. Also, a coal mine's environment is under the influence of a graduated, nonuniform, biaxial stress field controlled by gravity. It is necessary to consider all of these factors to validate the FMA. Previous research demonstrates the accuracy of the FMA by comparing it to numerical modeling output [Kramer 1996]. It is shown that the technique matches the numerical modeling predictions with a high degree of accuracy.

Figures 2 through 7 are plots that compare the stress prediction of the FMA with that of numerical modeling. The purpose is to show how well the FMA can predict stress even in conditions less ideal than those used by Westergaard to derive equation 1. Such conditions are similar to those encountered in an underground coal mine. All of the evaluations use FLAC[5] as the numerical modeling software. Spreadsheet graphs are used to compare the FMA stress prediction with that determined by FLAC. Each demonstrates that the FMA compares reasonably well with the FLAC model for varying conditions of nonhomogeneity. Initially, the model is homogeneous and simple. The FMA matches extremely well with the numerical model [Kramer 1996]. Then, in order to introduce nonhomogeneity into the numerical model, each individual structural property is altered independently and the results are compared with the FMA. Finally, an evaluation is made between the FMA and a nonhomogeneous numerical model consisting of strata with properties even more variant than an actual mine environment.

Figure 2 charts the comparative stress predictions between the FMA and FLAC for a simple, elastic, and homogeneous model. Note that the stress distributions are nearly exact. The only real difference is at the edge of the mine opening. This difference is due to the approximation technique used in numerical analysis. The model in figure 3 has the same homogeneous properties as those for figure 2; it plots the stress distribution through various planes in the coal seam. This illustrates that the distribution, at any plane, remains consistent with the distribution through the center plane of the seam. Figures 4 and 5 demonstrate that the coal's modulus of elasticity or Poisson's ratio has little effect on the stress distribution through the center plane of the coal seam. The next step is to compare the accuracy of the FMA for predicting the stress of a nonhomogeneous numerical model. Figures 6 and 7 relate the results of the simulation.

Figure 6 shows the comparison between FLAC and the FMA for the stress distribution produced in a graduated, nonuniform, biaxial stress field similar to that encountered in an underground mine. For these studies, the horizontal stress is 0.3 times the vertical stress. The design of the model places the coal seam at a depth of 381 m. The structural parameters of the coal and rock are equivalent. This study also compares the Westergaard equation to the stress at various planes in the seam (figure 6).

It can be seen that the nonuniform stress field in the numerical model causes a deviation in stress from the Westergaard prediction; however, most of the difference is near the edge of the mine opening. In this portion of the mine rib, the coal is yielding. Analytical methods do not exist for predicting the stress distribution in this region. Introduced later in this paperis a method that uses field measurements to describe the stress distribution in the yield zone of a coal rib.

[5] Fast Langrangian Analysis of Continuum, Itasca Corp., Minneapolis, MN.

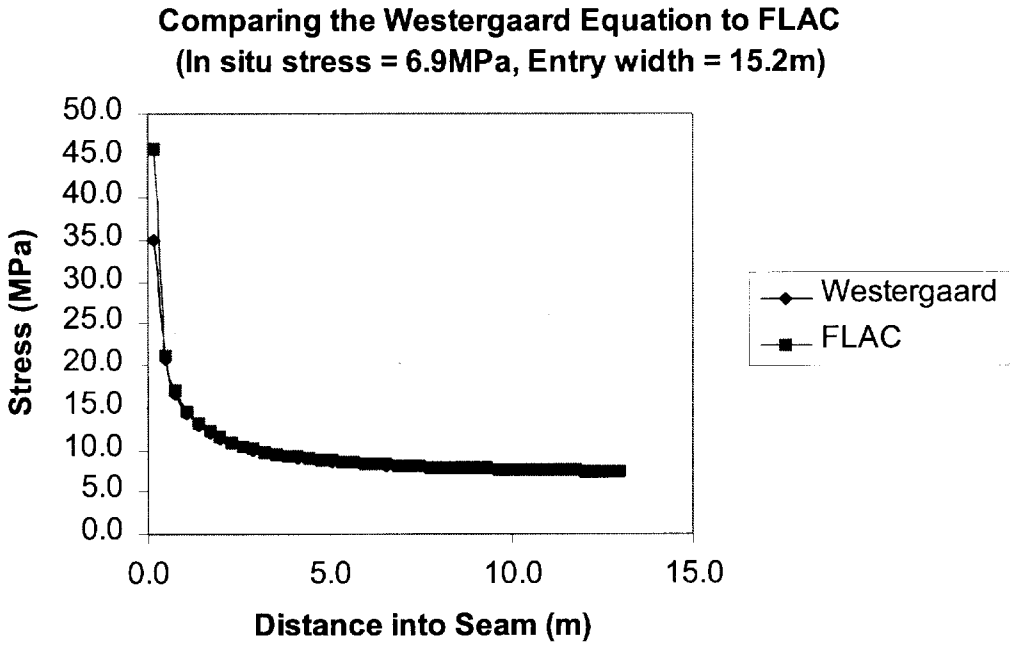

Figure 2.—Stress distribution in a coal seam next to a mine opening: comparison between numerical analysis and the Westergaard equation. Homogeneous model.

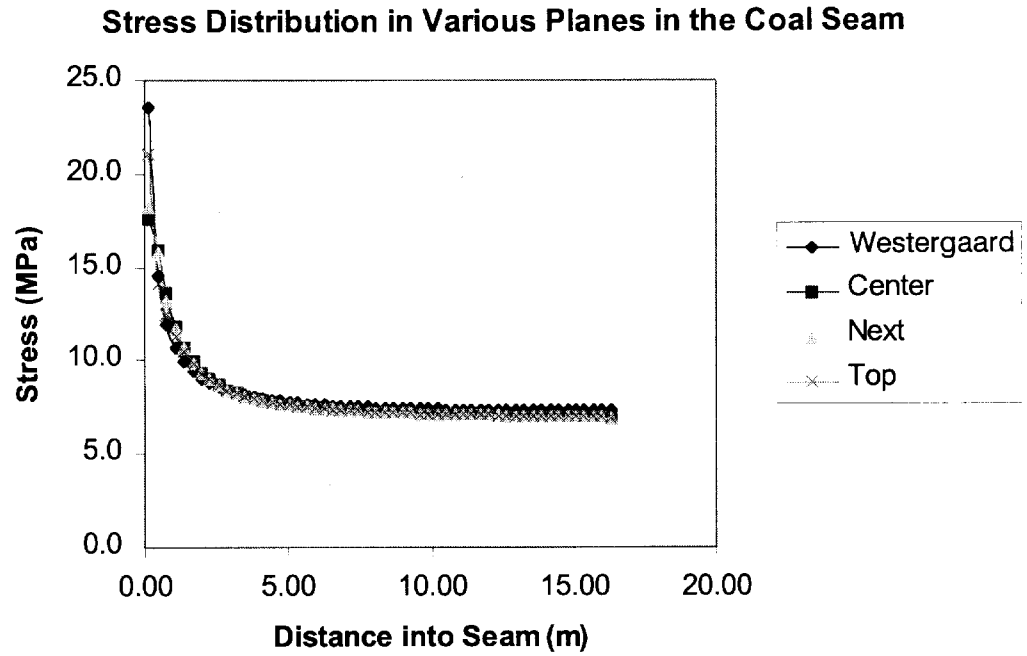

Figure 3.—Stress distribution at various levels in the coal seam. Properties similar to the model in figure 2.

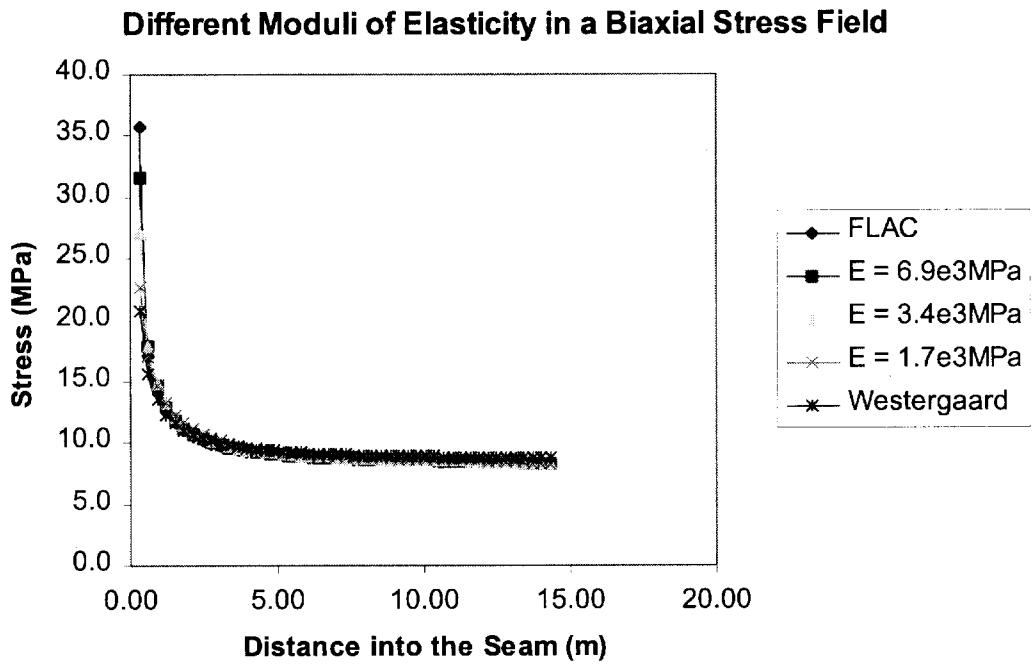

Figure 4.—Stress profile for coal with different moduli. Four separate FLAC models.

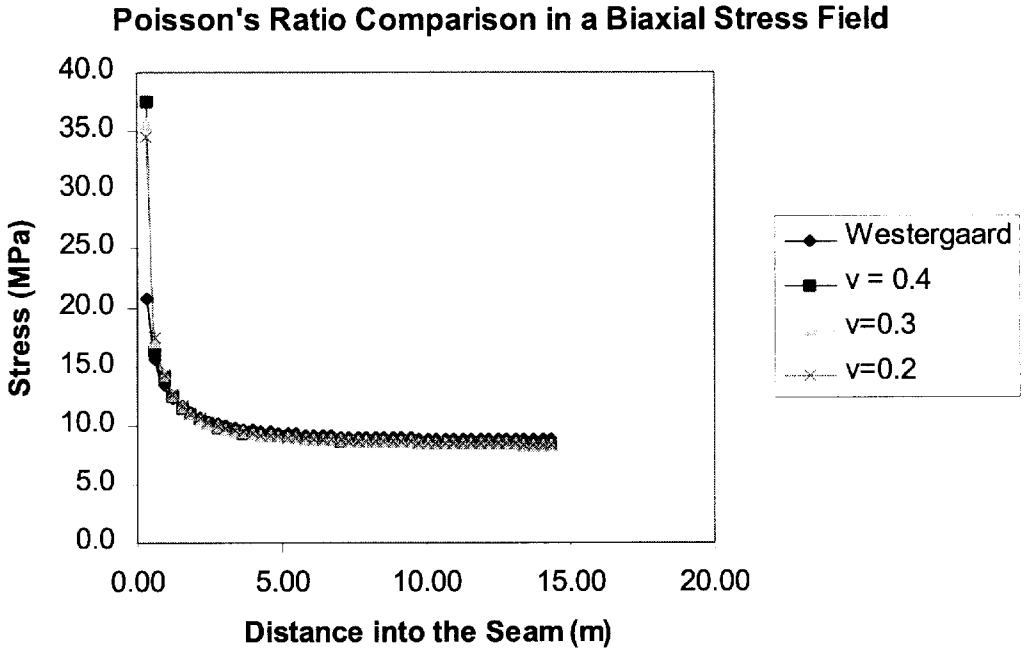

Figure 5.—How the Poisson ratio affects the stress distribution. Three separate FLAC models.

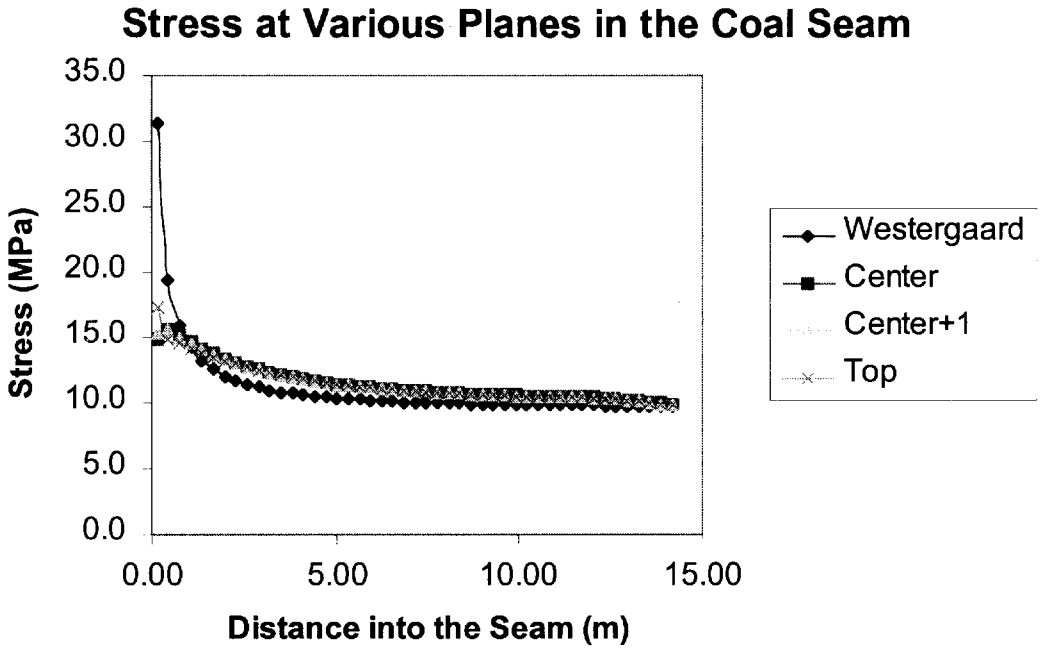

Figure 6.—The effect of a graduated, nonuniform biaxial stress distribution similar to conditions underground. Stress profile at various levels in the seam.

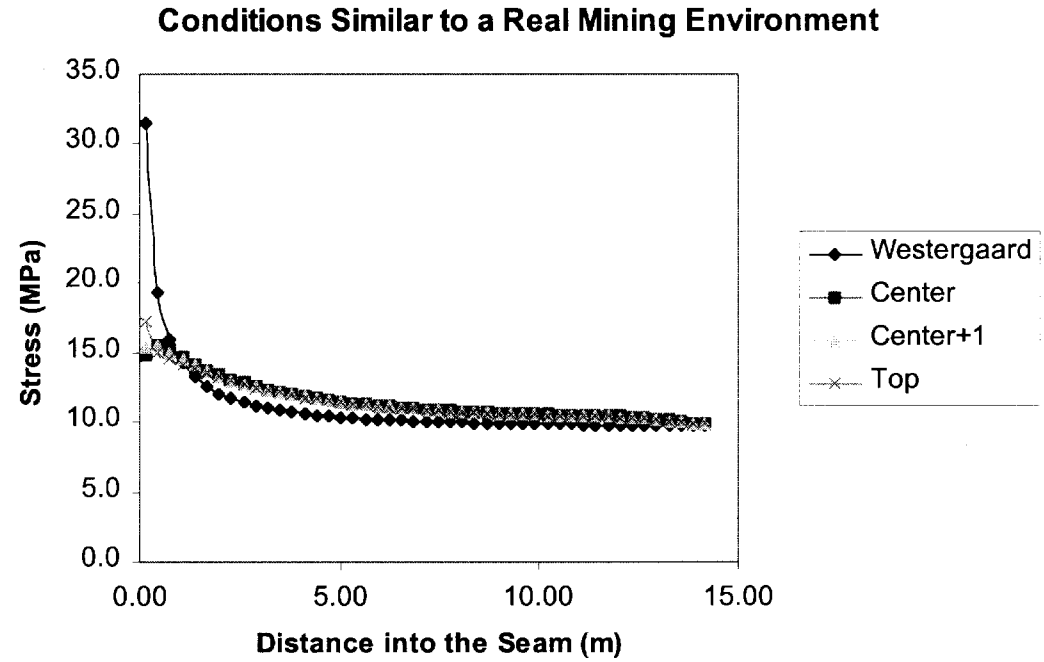

Figure 7.—Comparison of a model simulation of a real mine environment.

The numerical model described below will validate the FMA's ability to analyze structural variations found in a real mine environment. In this model, the strata are nonhomogenous. In addition, the surrounding stress field is variable in both the vertical and horizontal planes. Such a model has structural variations greater than those encountered in most coal mines. The surrounding rock mass has a Young's modulus of 27,580 MPa and a Poisson's ratio of 0.2. The unit weight of this mass is 0.03 MN/m^3. The coal seam has a Young's modulus of 3,448 MPa, a Poisson's ratio of 0.3, and a unit weight of 0.03 MN/m^3. The unit weights are high to enhance the stress comparisons by increasing the effect of gravity loading. To show the effect of mining in an area subjected to a high stress field, the model is initialized with a premining stress prior to adding the mine opening. Adding a mine opening to a model with a high biaxial stress field already in place would alter the stress in the areas adjacent to the mine opening. Figure 7 compares the Westergaard equation to FLAC's analysis for different levels in the coal seam. The distributions vary considerably; however, most of this deviation is near the mine opening. In this area, the coal will yield. A technique will be presented in this paper that describes the stress distribution in the yield zone of the coal.

THE POINT-FORCE METHOD USED TO SIMULATE MINE SUPPORTS

An essential concept of the FMA is the process by which a point force, acting on the surface of the crack, affects the stress intensity at the crack tip. In mining, this point force could be a mine post or hydraulic jack. A continuous series of point forces can model a yield pillar, longwall gob, the yield zone of the pillar, or any other type of mining supports [Kramer 1996]. Figure 8 depicts a crack with an internal point force, P, pushing out against the crack surface. This force P is at a distance x from the crack center. This force affects the stress intensity factor K at points A and B. The point force is similar to the loading from a single-point mine support, such as a post or hydraulic jack.[6]

Green functions are used to predict the stress intensity factors [Paris and Sih 1965]. The factors are:

$$K_A = \frac{P}{\sqrt{Ba}} \sqrt{\frac{a+x}{a-x}} \qquad (2)$$

$$K_B = \frac{P}{\sqrt{Ba}} \sqrt{\frac{a-x}{a+x}} \qquad (3)$$

where K_A = stress intensity at point A,

K_B = stress intensity at point B,

P = point force,

a = 1/2 the opening width,

and x = distance from opening center

[6]The stress intensity factor is of utmost importance in the study of fracture mechanics. It is a measure for the stress singularity at the crack tip. For the case of uniaxial compression with force P at infinity, K must be proportional to P. K_A and K_B must also be proportional to the square root of a length. For an infinite object, the only characteristic length is the crack size; thus, K must take the form: $K = F/(Ba)$.

YIELD PILLARS

Yield pillars are common in longwall mining; they control floor heave and/or fine tune roof behavior. As the name implies, the pillars yield, thus redistributing the load around a control area in the mine. It is possible to model yield pillars as a continuous series of point forces. Equations derived from in situ pillar strength measurements can determine the intensities of the point forces. However, for the present discussion, the point forces are considered uniform and equal to the yield strength of the coal (figure 9).

To illustrate the method, it is necessary to discuss only the stress effect at a single crack tip (e.g., point A in figure 9). Either equation 2 or equation 3 can describe the stress intensity at point A. The correct equation to use depends on the location of the point forces with respect to the a-origin. In the discussion below, the location of the point forces (figure 9) is chosen to provide the most complete example of the technique. Because the locations of the point forces are equally distributed on both sides of the origin, solution to the stress effect at point A requires using a combination of equations 2 and 3. In

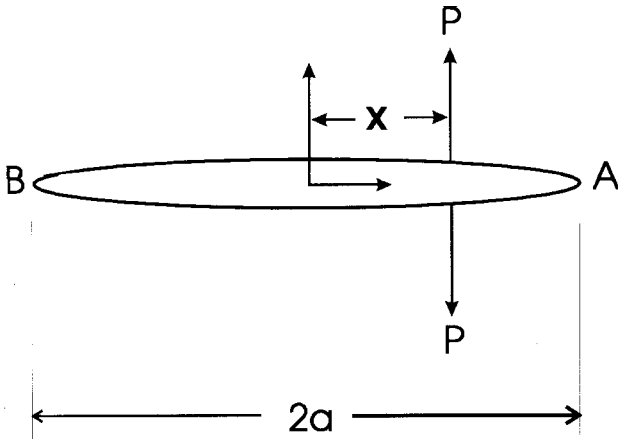

Figure 8.—Crack with wedge forces at x.

absence of the yield pillar, the stress intensity at point A is [Dugdale 1960]:

$$K_{insitu} = F_{insitu}\sqrt{Ba}\,. \tag{4}$$

The yield pillar will act to reduce this intensity. The a-origin is located in the center of the point forces; thus, the distribution in the &x side is equal to the distribution in the %x side (figure 9). The stress intensity factor at point A caused by the continuous point forces on the %x side of the origin is

$$K_{\%x} = K_A = \frac{F_{ys}}{\sqrt{Ba}} \int_0^d \sqrt{\frac{a\%x}{a\&x}}\,dx\,. \tag{5}$$

The stress intensity factor at point A caused by the continuous point forces on the &x side of the origin is

$$K_{\&x} = K_A = \frac{F_{ys}}{\sqrt{Ba}} \int_0^d \sqrt{\frac{a\&x}{a\%x}}\,dx\,. \tag{6}$$

The stress intensity factor for the yield pillar becomes

$$K_{yield} = K_{\%x} \% K_{\&x}. \tag{7}$$

With the yield pillar in place, the stress intensity factor at point A becomes

$$K_{total} = K_{insitu} \& K_{yield}. \tag{8}$$

The Westergaard equation relates rib stress to the in situ stress and the width of the opening. Because K_{total} includes not only the in situ stress but also the effect of the yield pillar, it is necessary to modify the Westergaard equation to reflect this effect. It is necessary to modify the Westergaard equation by substituting a dummy variable in place of a real variable. The opening half-width variable "a" is the proper choice for the substitution.[7] Solving for "a" in K_{total} and substituting it into the Westergaard equation as a dummy variable will provide the proper stress distribution at point A. The following demonstrates the concept.

The stress intensity factor is defined as

$$K = F\sqrt{Ba}\,. \tag{9}$$

To modify the Westergaard equation, it is necessary to substitute values and solve for the unreal "a", making it a dummy variable such that

$$a_{dummy} = \frac{K_{total}^2}{BF_{insitu}^2}\,. \tag{10}$$

The reduced Westergaard stress distribution at point A then becomes

$$F_{modified}(x) = \frac{F_{insitu}\,x}{\sqrt{x^2 \& a_{dummy}^2}}\,. \tag{11}$$

[7]Modifying F would result in the stress distribution leveling to a value below the in situ stress.

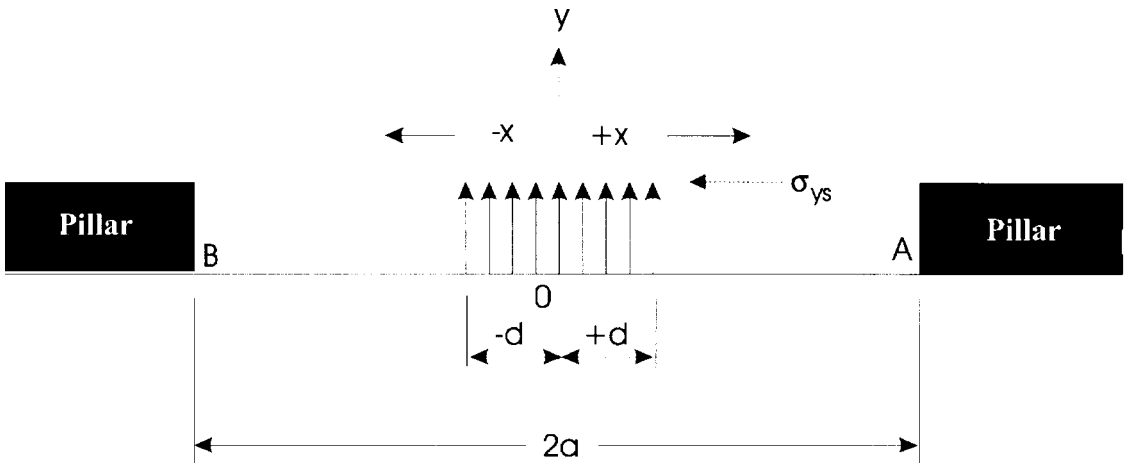

Figure 9.—Yielded pillar modeled as a continuous set of point forces.

LONGWALL GOB

The technique used to model longwall gob is similar to that for the yield pillar. An assumption can be made that the center of the gob is in contact with the roof and floor and the material is compacted completely. Due to symmetry, it is necessary to model only one-half the gob width to determine its effect on the stress intensity at the tip of the opening. Therefore, the opening extends from the gob center to edge of the gate pillar at point A (figure 10). The residual strength of this material is a function of the amount of compaction. Because the center of the gob has the greatest compaction, it has the greatest residual strength; the outside edge of the gob has the least. To simulate gob material, the point forces are high in the center of the gob and low at the edge. Originally, the following example was formulated using U.S. customary units of measurement. Conversion to the metric system makes some values appear awkward.

As usual, the a-origin and x-origin begin at a point equidistant from point A and the gob center. The point forces to the right of the origin (i.e., %x side) would use equation 5 to analyze the effect at point A; the point forces to the &x side of the origin will use equation 6. "Derive—A Mathematical Assistant"[8] is used to solve for the integral in each equation. Included in table 1 are the input variables and resultant stress intensity factors for the gob depicted in figure 10. The gob material in the model is divided into six sections, each reflecting a different yield strength (YS_1 to YS_6). The first three sections are in the &x side (K_B side) of the origin; the other three are in the %x side (K_A side). The location of the section determines which point-force equation to use. The total effect of the gob is the summation of the K-values for all six sections:

$$K_{gob} = K_1 + K_2 + K_3 + K_4 + K_5 + K_6. \qquad (12)$$

This value is subtracted from the K_{insitu} value (the stress intensity for the large opening without the gob material in place) to obtain the proper stress intensity factor at point A. The relation is

$$K_{total} = K_{insitu} - K_{gob}. \qquad (13)$$

EXAMPLE

Below is an example that demonstrates the technique. It analyzes the effect from two sections of the complete model shown in figure 10. These particular sections (sections 3 and 4) were chosen to illustrate forces on either side of the axis origin. The point forces in section 3 align in the &x direction; those in section 4 are in the %x direction. The stress intensity factor will be determined using a combination of equations 5 and 6. Table 1 lists the results from the complete analysis.

[8]Derive—A Mathematical Assistant," Soft Warehouse, Inc., 3660 Waialae Ave., Honolulu, HI.

Input Parameters:

Width of longwall face = 232 m
1/2 width of longwall face = 116 m
2a (width of longwall face plus gate entry) = 122 m
a = 61 m
F_{insitu} = 13.8 MPa

Section 3:

The yield strength for section 3 is F_{ys3} = 12.4 MPa. It occupies the &x portion of the a-axis for the 0- to (&)18.3-m segment. The effect on the stress intensity at point A due to section 3 of the gob is

$$K_3 = \frac{F_{ys}}{\sqrt{Ba}} \int_0^{18.3} \sqrt{\frac{a - x}{a + x}}\, dx$$

$$= \frac{12.4}{\sqrt{B61}} \int_0^{18.3} \sqrt{\frac{61 - x}{61 + x}}\, dx$$

$$= 14.1$$

NOTE: Although the point forces are in the -x region, the limits of the integral are from 0 to (%)18.3 m.

Section 4:

The yield strength for section 4 is F_{ys4} = 10.3 MPa. This section occupies the %x portion of the a-axis for the 0- to (%)18.3-m segment. The effect on the stress intensity at point A due to section 4 of the gob is

$$K_4 = \frac{F_{ys}}{\sqrt{Ba}} \int_0^{18.3} \sqrt{\frac{a + x}{a - x}}\, dx$$

$$= \frac{10.3}{\sqrt{B61}} \int_0^{18.3} \sqrt{\frac{61 + x}{61 - x}}\, dx$$

$$= 15.9$$

"Derive—A Mathematical Assistant" solved both of these integrals. The solutions yield a rather cumbersome equation that is impractical to include in this paper; however, it can be incorporated into spreadsheet software or computer code. Table 1 includes the K factors for all six sections of the longwall gob. The effect on the stress intensity factor at point A caused by all six sections is

$$K_{gob} = K_1 + K_2 + K_3 + K_4 + K_5 + K_6$$
$$K_{gob} = 13.8 + 10.7 + 14.1 + 15.9 + 18.0 + 25.8$$
$$K_{gob} = 98.3$$

Table 1.—Input variables and stress intensity factors for each section of the longwall panel depicted in figure 10

	Section 1	Section 2	Section 3	Section 4	Section 5	Section 6
F_{ys}, MPa	13.8	13.1	12.4	10.3	8.3	6.9
x-range, m	61.0-36.6	36.6-18.3	18.3-0	0-18.3	18.3-36.6	36.6-55.0
Stress intensity at point A (%x side)	—	—	—	15.9	18.0	25.8
Stress intensity at point A (&x side)	13.8	10.7	14.1	—	—	—
K_{gob}	98.3	—	—	—	—	—

Input parameters:
Width of longwall face ' 232 m
1/2 width of longwall face ' 116 m
2a (width of longwall face plus gate entry) ' 122 m
a ' 61 m
F_{insitu} ' 13.8 MPa

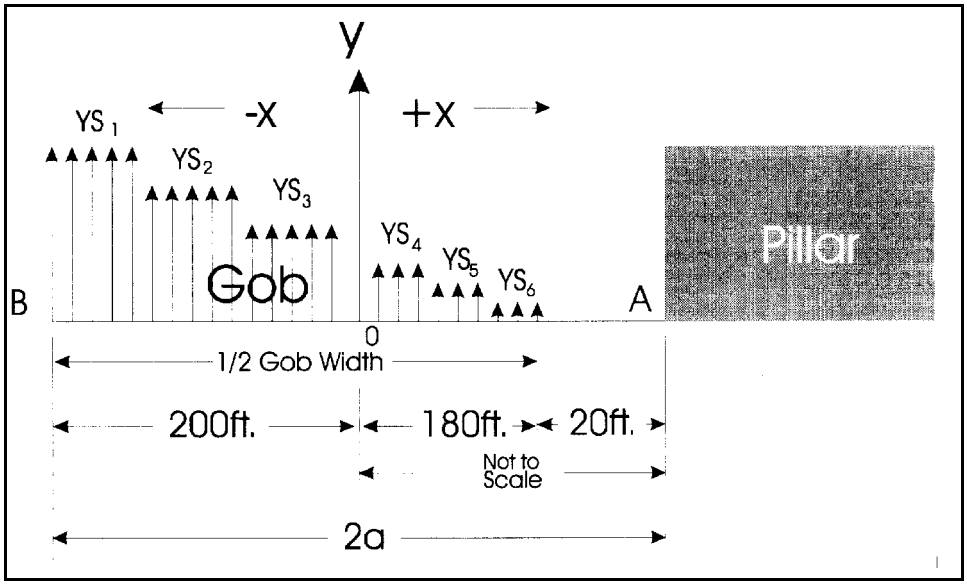

Figure 10.—Longwall gob simulated as point forces of different strengths.

Equation 4 determines the stress in absence of the gob (point forces) as

$$K_{insitu} ' F_{insitu}\sqrt{Ba}$$

$$K_{insitu} ' 13.8\sqrt{B61}$$

$$K_{insitu} ' 191.0$$

It is necessary to reduce this intensity to reflect the addition of the gob material. The stress intensity factor at point A now becomes

$$K_{total} ' K_{insitu} \& K_{gob}$$
$$K_{total} ' 92.7$$

The dummy variable used to relate this stress reduction to the Westergaard equation is

$$a_{dummy} ' \frac{K^2_{total}}{BF^2_{insitu}}$$

$$a_{dummy} ' \frac{(92.7)^2}{B(13.8)^2}$$

$$a_{dummy} ' 14.4 \text{ m}$$

The modified Westergaard distribution at point A becomes

$$F_{modified}(x) ' \frac{F_{insitu}x}{\sqrt{x^2 \& a^2_{dummy}}}$$

$$F_{modified}(x) ' \frac{13.8x}{\sqrt{x^2 \& 14.4^2}}$$

This is the general technique used to model longwall gob. Luo significantly improved the above technique and developed a computer program to model the stability of longwall chain pillars [Kramer et al. 1998].

HYDROSTATIC FORCES

It is possible to measure the effect of hydrostatic forces on the coal seam. A hydrostatic force acts with equal strength in all three cardinal directions. It is similar to the pressure exerted from water or gas. To simulate a hydrostatic force, it is necessary to fill the entire mine opening with a continuous distribution of point forces (figure 11). In order to test the hydrostatic effect, the point forces are set equal to the in situ stress (13.8 MPa). This situation should have the effect of flattening the stress distribution at point A to a level equal to the in situ stress.

Figure 12 is a plot of the stress distribution. It can be seen the distribution is almost uniform and equivalent to the in situ stress. This further demonstrates that the point-force method accurately describes the effective stress distribution at the mine rib.

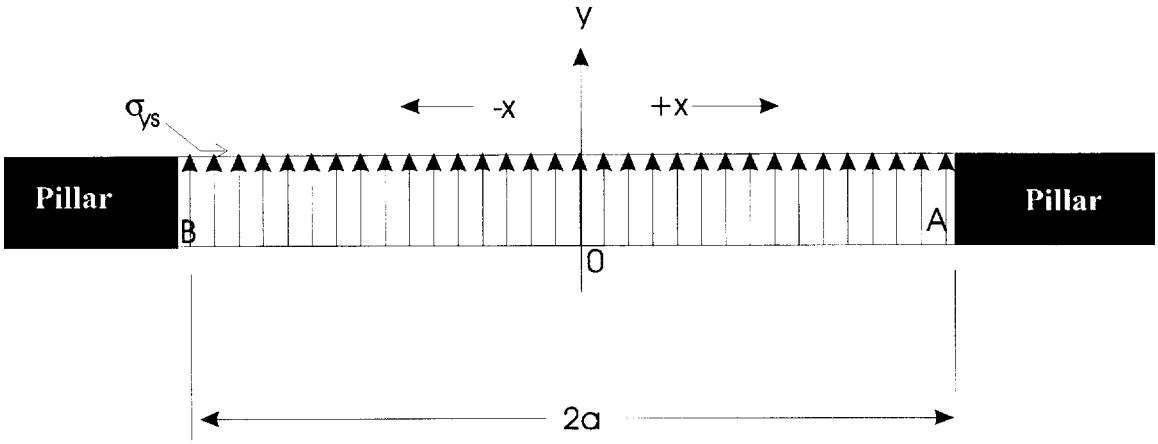

Figure 11.—Crack opening completely filled with point forces equal to the in situ stress.

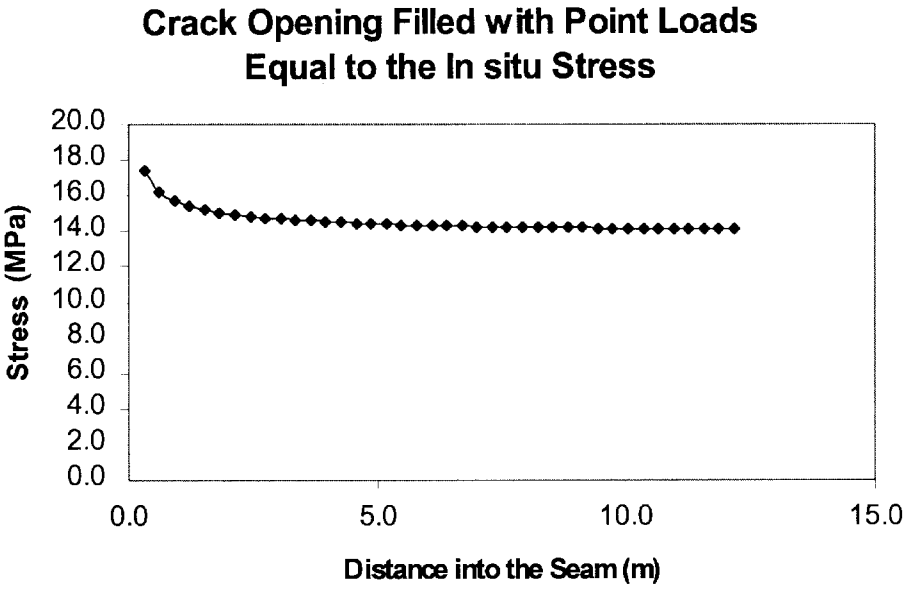

Figure 12.—Stress distribution at point A is nearly flat and equal to the in situ stress.

TECHNIQUE TO COMBINE DIFFERENT MINE SUPPORTS

It is possible to combine any type of mine supports and predict the resultant stress distribution in the coal seam. Figure 13 presents a typical mining environment combining the following structures: a longwall gob, a yield pillar, and a crib. Analyzing this arrangement requires a combination of the stress intensity factors for each support member. This combined value is used to reduce the total stress intensity at point A. The procedure for doing this is as follows:

- Calculate K_{insitu} for point A
- Calculate K_{gob} for point A
- Calculate K_{yield} for point A
- Calculate K_{crib} for point A
- Combine the stress intensity factors for each support, and use this value to reduce the stress intensity associated with the entire opening width:

$$K_{total} = K_{insitu} + K_{gob} + K_{yield} + K_{crib}$$

EVALUATING PILLAR YIELD

Because coal mines are often located at a great depth below the surface, the stress levels often exceed the yield strength of the coal. It is necessary to account for yielding in the coal pillars to correctly assess structural stability. Fracture mechanics is useful in predicting the yielding characteristics of the coal.

The Westergaard equation introduces a singularity at the pillar edge. This is where the stress distribution approaches infinity. The pillar edge yields and redistributes the loading in order to eliminate the singularity. The yielded zone continues to offer residual support to the roof and floor.

Dugdale provides a way to estimate the length of this yield zone in the pillar [Dugdale 1960; Broek 1982]. The following sections describe how to determine the extent of the yield zone. Also described is a way to predict the stress distribution in the elastic core of the pillar. First, the basic technique used by Dugdale to arrive at his yield zone prediction is reviewed. Later, a technique is introduced that determines the extent of the yield zone specifically in coal.

THE EFFECT OF POINT LOADING ON THE STRESS INTENSITY AT THE CRACK TIPS

As mentioned previously, figure 8 depicts a crack with an internal wedge force P pushing out against the crack surface. This force P is at a distance x from the crack center. These wedge forces affect the stress intensity function, K, at points A and B. It is possible to use equations 2 and 3 to predict these stress intensity factors, K [Paris and Sih 1965]. A form of these equations is fundamental in the development of residual forces supporting the roof and floor in the yielded portion of the pillar.

DUGDALE'S APPROACH TO CRACK TIP YIELDING

Although the pillar edge yields, it has a residual strength that supports the roof and floor of the coal seam. Imagine this residual support as a continuous distribution of dislocated point forces (figure 14). Dugdale determined the extent of the yielded zone by first assuming that the residual strength of each point force is equal to the yield strength, F_{ys}, of a material (in this case, coal) [Dugdale 1960; Broek 1982]. Because the yielded edge is significantly weaker, it would seem as though the mine opening becomes wider. The mine opening would theoretically extend into the pillar to the point where yielding stops. At this point, the singularity disappears because of the canceling effect of the residual stress in the yield zone. The effective mine width, $a_{eff} = a + D$, represents the distance to the new elastic crack tip, where D symbolizes the extent of the yielded zone.

The yielded zone, D, exerts a residual stress equal to the yield stress, $F_{ys.}$ The yield zone, D, depicted as additional opening width, is not really an opening; the material can still bear the yield stress. The size of D is chosen so that the stress singularity disappears: K_{total} approaches zero. This means that the stress intensity, K_{insitu}, due to the uniform in situ stress, F, has to be compensated by the stress intensity, K_D, due to the residual wedge forces F_{ys} [Broek 1982]. In other words:

$$K_{insitu} = -K_D \tag{14}$$

Satisfying equation 14 leads to the determination of D in the following manner. Equations 2 and 3 describe how a point load affects the stress intensity factor, K. If the wedge forces are distributed from s to the effective crack tip, the stress intensity becomes

$$K = \frac{P}{\sqrt{Ba}} \int_s^a \left(\sqrt{\frac{a+x}{a-x}} + \sqrt{\frac{a-x}{a+x}} \right) dx . \tag{15}$$

Solution to this integral is

$$K = 2P\sqrt{\frac{a}{B}} \cos^{-1}\frac{s}{a} . \tag{16}$$

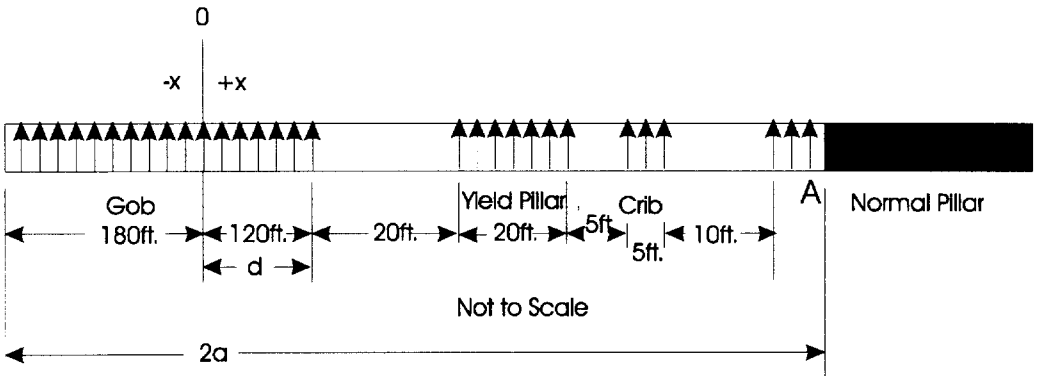

Figure 13.—Modeling various support structures using the point-force technique.

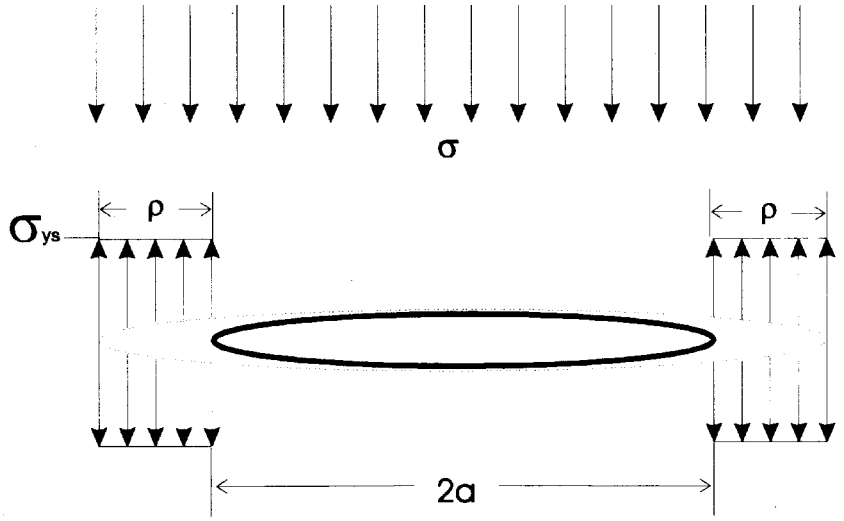

Figure 14.—Continuous point forces approximate the residual pillar strength in yielded zone preceding the elastic crack tip.

Applying this result to the crack in figure 14, the integral has to be taken from s ' a to a ' a % D. Thus, "a" has to be substituted for "s" and "a % D" for "a" in equation 16, while P equals the yield strength, F_{ys} [Broek 1982]. This leads to the determination of the yield zone as

$$D ' \frac{B^2F^2a}{8F_{ys}^2}, \qquad (17)$$

where D is the extent of the pillar yield zone.

Dugdale's description of the yield zone does not provide a simple way to predict the stress distribution in the elastic core adjacent the yielded edge. Irwin presents a method to predict the stress distribution in the elastic portion of the pillar [Broek 1982]. Irwin describes a yield zone that is similar in length to Dugdale's prediction; however, the crack tip extends only one-half the distance (figure 15).

The singularity vanishes if area A ' area B. It was possible to verify this using spreadsheet software. It is particularly accurate for values of F/F_{ys} less than 0.75. Irwin's description produces the stress distribution shown in figure 16. This distribution is not representative with in situ measurements taken at underground mines [Mark and Iannacchione 1992].

PLAIN STRAIN

Dugdale's method concerns conditions of plane stress. Pillar analysis requires a plane strain condition. Studies indicate that for the case of plain strain, the effective yield stress can be as great as three times that for a similar plain stress analysis. This is due to confinement, which increases the triaxial yield strength. Broek suggests modifying the yield stress with the constraint factor:

$$\text{p.c.f.} ' 1.68F_{ys} \qquad (18)$$

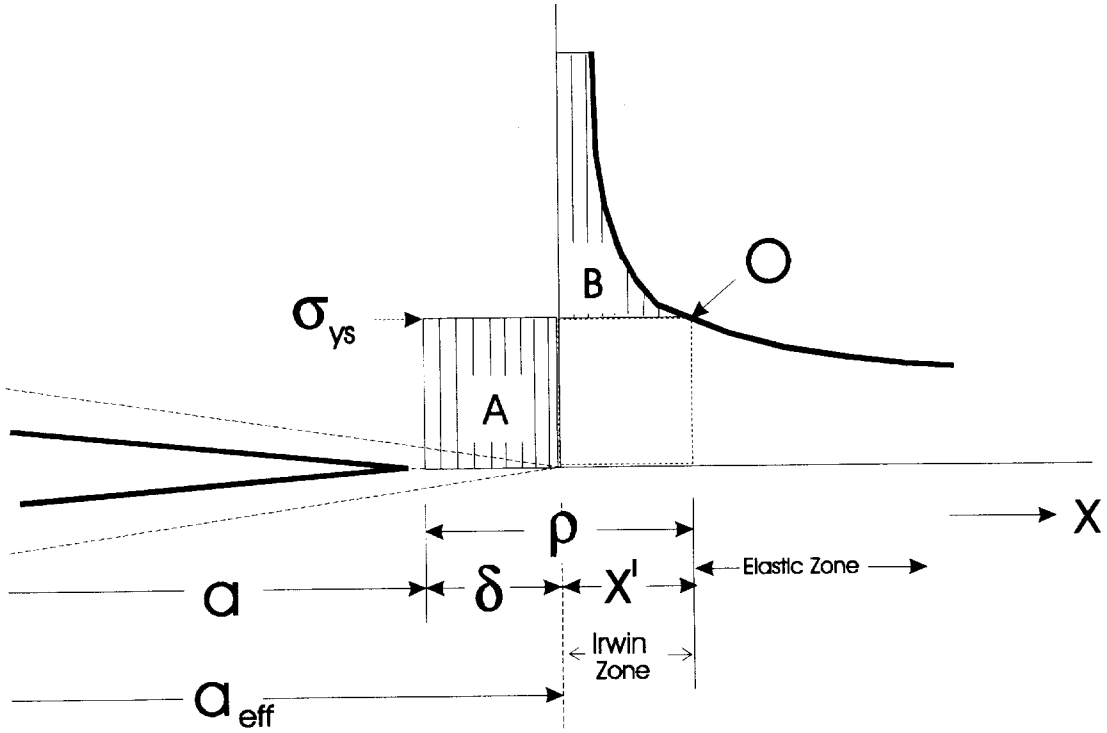

Figure 15.—The Westergaard distribution originates at the beginning of the Irwin zone, but does not take effect until the beginning of the elastic zone.

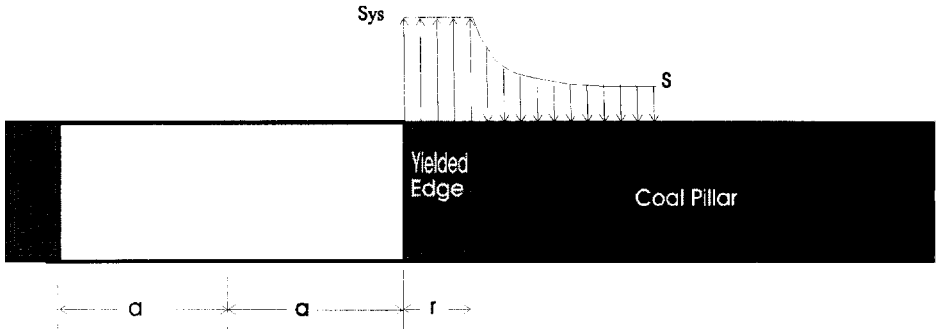

Figure 16.—Pillar stress distribution as predicted by the Dugdale-Irwin method.

THE DUGDALE-IRWIN METHOD AS IT RELATES TO A MINE ENVIRONMENT

Previous research indicates that confinement increases the yield strength of a pillar core [Crouch and Fairhurst 1973; Karabin and Evanto 1999; Sih 1966; Salamon and Munro 1967]. However, the measured pillar stress distribution does not resemble the distribution predicted by Dugdale-Irwin shown in figure 16. Underground measurements show the residual strength should be low at the wall of the mine opening, but increase proportionally with the distance into the pillar core.

The mathematical model predicted by Dugdale-Irwin is accurate; only the visual perception is misleading. The residual stress distribution in the yielded area can take on any shape as long as area A equals area B (figure 17). A more realistic stress distribution such as that in figure 18 should then be possible.

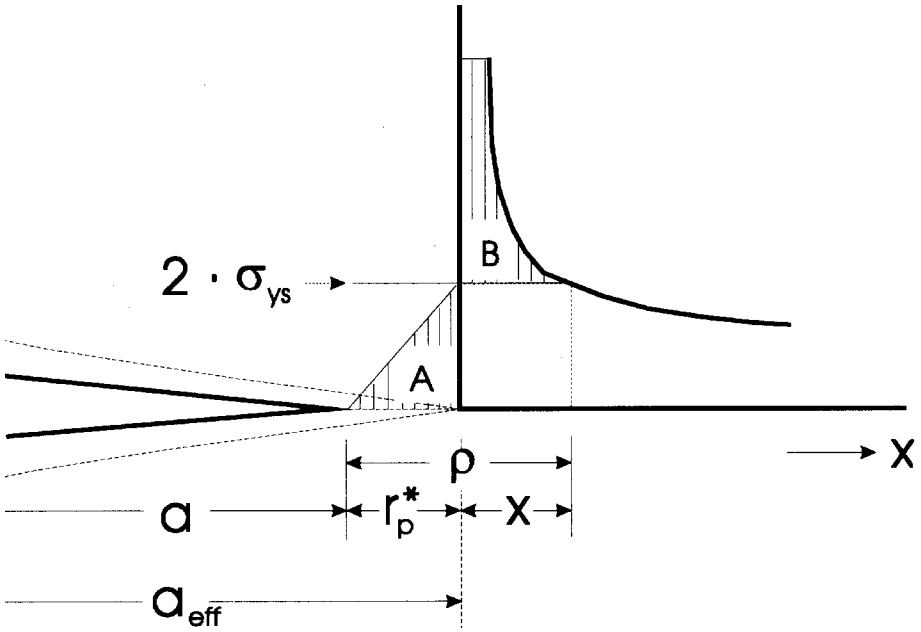

Figure 17.—Yield stress can assume any shape provided that area A equals area B.

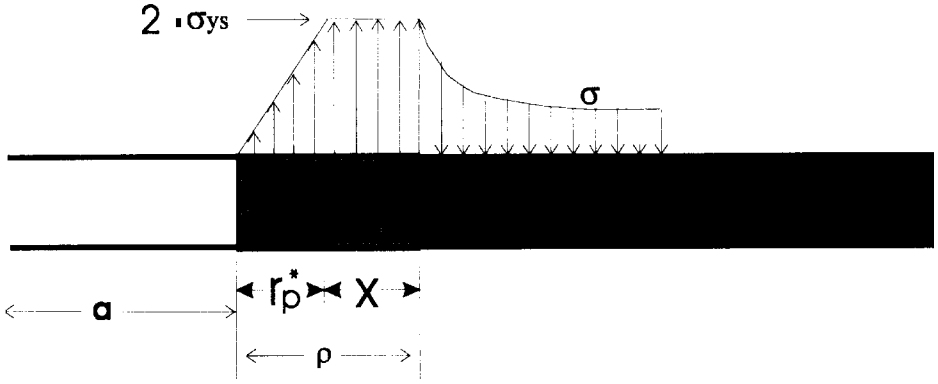

Figure 18.—Possible contour of pillar stress using the Dugdale-Irwin method.

COMBINING EMPIRICAL METHODS INTO THE ANALYTIC ANALYSIS

The Westergaard equation introduces a singularity at the pillar edge; this is where the stress approaches infinity. To eliminate this singularity, the edge must yield and redistribute the load. The yielded edge retains a residual strength that offers confinement to the core.

In situ field measurements demonstrate a nonlinear residual stress distribution in the yield zone of a coal pillar. The stress is low at the pillar rib and increases rapidly into the center of the pillar. This indicates that confinement makes the pillar strength higher than the unconfined compressive strength used by Dugdale-Irwin. It is possible to use the point-force method to model this residual strength and thus predict the extent of the yield zone. It is a common numerical technique to study the yielding coal with a strain-softening model [Crouch and Fairhurst 1973; Wilson 1972]. Figure 19 depicts a model in terms of stress versus strain in a timeframe denoted by peak and post (residual) stress.

It is possible to use any of the popular pillar strength equations to predict the strain-softening characteristics of the coal. The equations of Bieniawski and Holland-Gaddy are the most accepted of these equations [Mark and Iannacchione 1992]. Mark and Iannacchione developed an equation that represents an average of these two equations. It predicts the pillar strength as a function of distance from the opening. This equation is:

$$F_v(x) = S_1 \times \left(0.78 + 1.74 \frac{x}{h} \right), \qquad (19)$$

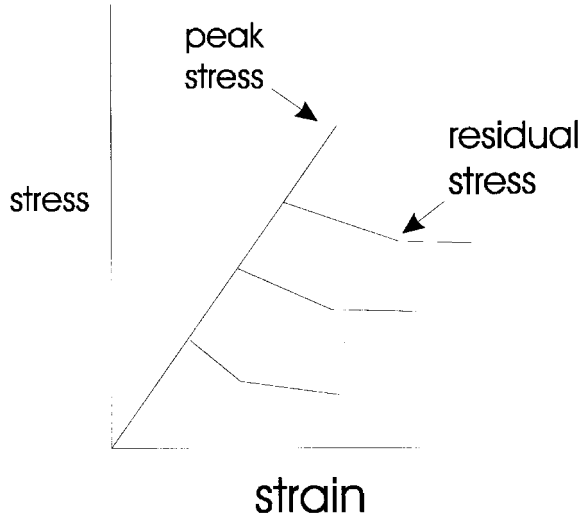

Figure 19.—The stress-strain characteristics in the yield zone of a coal seam.

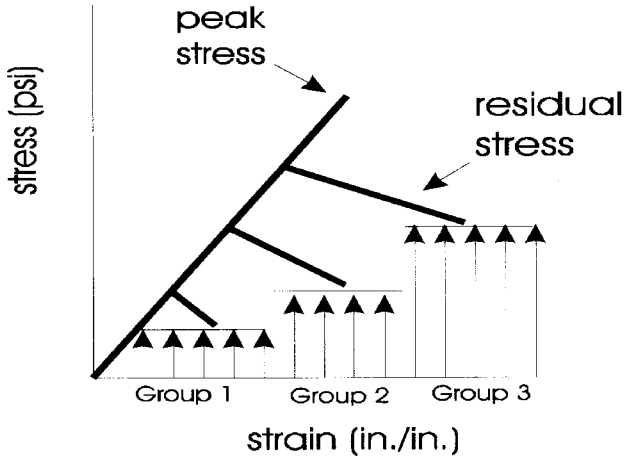

Figure 20.—It is possible to model peak or post stress as several groups of point forces.

where F_v = peak stress at distance x, MPa,

S_1 = in situ coal strength, MPa,

x = distance to the free face, m,

and h = seam height, m.

It is possible to model the stress distribution in the yield zone as a series of point forces (figure 20). These continuous series of point forces has a uniform intensity within each group. Equation 19 will predict the average strength assigned to each group. It is necessary to use an iterative technique to determine the extent of the yield zone. This iterative technique progressively yields each group while testing for the disappearance of the singularity. When $K_p \geq K_{insitu}$, the yielding stops. Luo has eliminated the need for an iterative technique by providing the exact solution for the equation [Kramer et al. 1998].

EXAMPLE: USING STRAIN-SOFTENING TO DETERMINE THE EXTENT OF THE YIELD ZONE

Originally, this example was formulated using U.S. customary units of measurement. Conversion to the metric system makes some values appear awkward.

GROUP 1: 0-2 m INTO THE PILLAR

Input Parameters:

$S_1 = 3.5$ MPa
$F_{insitu} = 6.9$ MPa
Entry width (2a) = 6 m
a = 3 m
Extension of group 1 (e_1) = 2 m
h = 2 m
$a_{eff1} = a + e_1 = 5$ m

The first group of point forces simulates the post strength for group 1, which is the first 2 m into the pillar (figure 20). These point forces are uniform; therefore, it is necessary to use equation 19 to determine an average strength value. This value will be assigned the point forces in group 1. An estimate of the average point force for group 1 would be determined from equation 19 for a point 1 m into the pillar.

$$F_{avg} = F_v(1\,m) = 3.5\left(0.78 + 1.74\,\frac{1}{2}\right) = 5.8 \text{ MPa}$$

The stress intensity relating to this average point force is taken from equation 15 as

$$K_{ps_{1,1}} = \frac{F_{avg}}{\sqrt{Ba_{eff}}} \int_a^{a_{eff}} \left(\sqrt{\frac{a_{eff} + x}{a_{eff} - x}} + \sqrt{\frac{a_{eff} - x}{a_{eff} + x}} \right) dx .$$

Equation 16 solves this integral as

$$K_{ps_{1,1}} = 2F_{avg}\sqrt{\frac{a_{eff}}{B}}\cos^{-1}\frac{a}{a_{eff}}$$

$$K_{ps_{1,1}} = 2\left(5.8\sqrt{\frac{5}{B}}\cos^{-1}\frac{3}{5}\right.$$

$$= 13.6$$

$$K_{ps_{total}} = K_{ps_{1,1}}$$

$$= 13.6$$

The stress intensity for group 1 in absence of the point forces is

$$K_{a_{eff1}} = 6.9\sqrt{B(3+2)}$$

$$= 27.3$$

$K_{ps\ total}$ is less than K_{aeff1}; therefore, this section is yielded and the crack extends to the end of the next section (group 2). The coal continues to yield until the residual pillar stress overcomes the in situ Westergaard stress.

GROUP 2: 2-4 m INTO THE PILLAR

Input Parameters:

$e_2 = 2$ m
$a_{eff1} = 5$ m
$a_{eff2} = a_{eff1} + e_2 = 7$ m
Midpoint of group 2 is 3 m into the pillar

The crack tip is extended 4 m (i.e., $e_1 + e_2$) to the end of group 2. This makes a_{eff2}, the effective crack tip, equal to 7 m. Using equation 19, the average stress in this section is 11.9 MPa. This is the post strength determined for a location 3 m into the pillar. The stress intensity caused by the wedge forces in group 2 is

$$K_{ps_{2,2}} = 2\left(11.9\sqrt{\frac{7}{B}}\cos^{-1}\frac{5}{7}\right.$$

$$= 27.5$$

It is necessary to also consider the stress intensity caused by the residual point forces in group 1. Because the crack tip extended into the 2-to 4-m (group 2) section of the yield zone, it is necessary to recalculate the effect of the 0- to 2-m (group 1) section of the yield zone:

$$K_{ps_{1,2}} = \frac{5.8}{\sqrt{B7}}\int_3^5\left(\sqrt{\frac{7+x}{7-x}}+\sqrt{\frac{7-x}{7+x}}\right)dx$$

"Derive—A Mathematical Assistant" determined this value to be:

$$K_{ps_{1,2}} = 6.1$$

The total stress caused by the point forces is

$$K_{ps_{total}} = K_{ps_{2,2}} + K_{ps_{1,2}}$$

$$= 33.6$$

The stress intensity caused by the crack extension to the end of group 2 in absence of the residual point forces is

$$K_{a_{eff2}} = 6.9\sqrt{B(5+2)}$$

$$= 32.3$$

This stress factor is less than the stress intensity due to the residual strength point forces ($K_{aeff2} < K_{ps\ total}$); thus, the yielding ceases in group 2. Because the values are nearly equal, the crack extended almost to the end of group 2 (i.e., 4 m into the pillar). It is possible to refine this distance, but it is unnecessary for this example. Equation 19 will predict the stress distribution in the yield zone; the Westergaard equation will predict the distribution in the elastic core.

Irwin suggests a way to use the Westergaard equation to predict the stress distribution in the pillar's elastic core (at the edge of the yield zone) [Broek 1982]. Irwin agrees with Dugdale's prediction for the extent of the yield zone, but he argues that the crack tip extends into this zone one-half the distance predicted by Dugdale such that

$* = D/2 = 2$ m (in the previous example).

This increases the effective crack width to

$$a_{eff} = a + * = 5 \text{ m}.$$

This is the beginning of the Irwin zone—the region from which the Westergaard equation predicts the stress distribution into the core of the material (figure 21).

Extending the crack tip to the beginning of the Irwin zone, the Westergaard equation becomes

$$F_{Irwin\ zone} = \frac{F_{insitu}x}{\sqrt{x^2-(a+*)^2}}. \qquad (21)$$

Although the x-origin in the Westergaard equation begins in the Irwin zone, the stress distribution does not take effect until the beginning of the elastic zone. Equation 19 describes the stress distribution throughout the entire yield zone. Figure 22 shows the stress distribution for the combined strain-softening and analytic models.

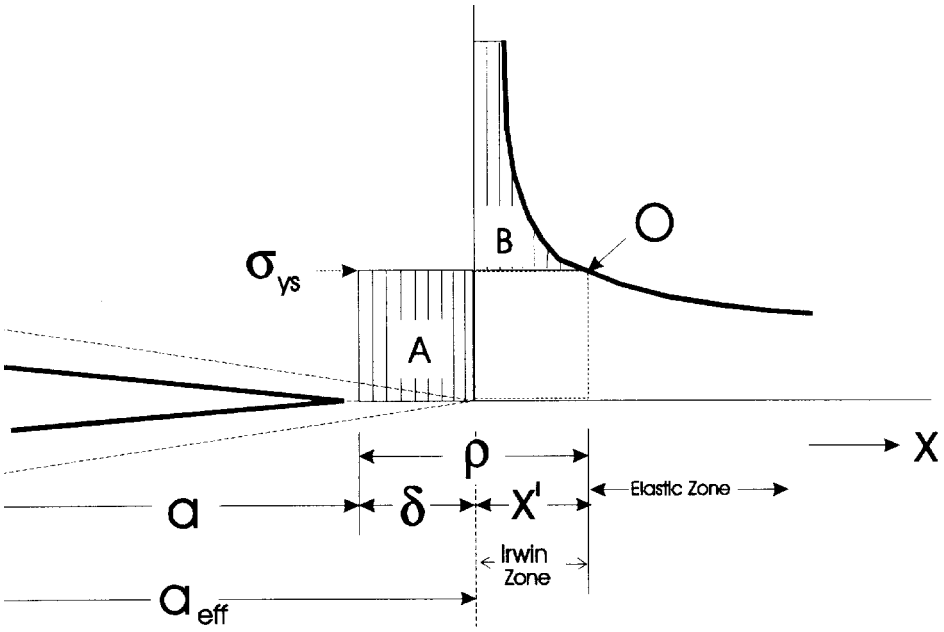

Figure 21.—The Westergaard equation begins in the Irwin zone; it takes effect in the elastic zone.

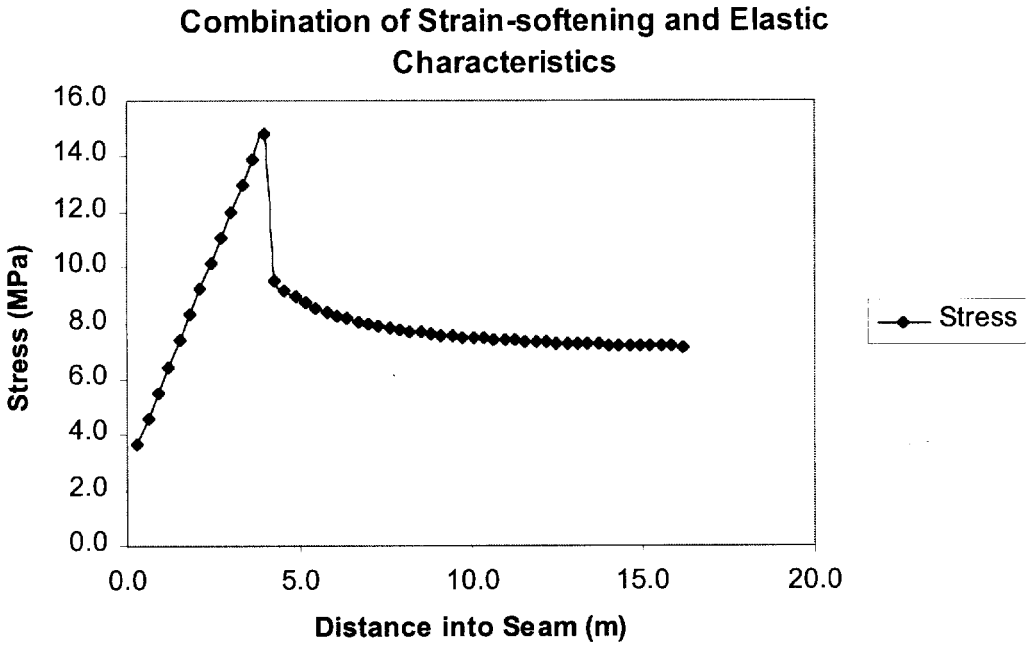

Figure 22.—Strain softening in the process zone and a Westergaard distribution in the elastic zone.

SUPERPOSITION

A mine opening affects the stress distribution at each of its sides. A mine panel is a gridwork of regularly or irregularly spaced entries and crosscuts.[9] For a complete stress analysis, it is necessary to consider the stress influences caused by every mine passageway. A superposition technique makes this possible [Kramer 1996].

The superposition technique requires subdividing the stress distribution into its constitutive components (figure 23). Each side of the pillar is subjected to a Westergaard stress distribution. Restricting the pillar model to two dimensions, as in the case of plane strain, limits these distributions to the left and right sides of the pillar. The basic components needed in the superposition are the uniform in situ stress, the stress component from the left opening, and the stress component from the right opening. The right and left stress components are each equal to the Westergaard equation with the in situ stress removed such that

$$F_{component} = \frac{F_{insitu} x}{\sqrt{x^2 - a^2}} - F_{insitu}. \qquad (22)$$

[9]An entry is a tunnel aligned in the main direction of mining. A crosscut connects individual entries, usually at a right angle. Several entries and crosscuts comprise a mine panel. A pillar is coal remaining in place between two entries and crosscuts; it supports the mine roof.

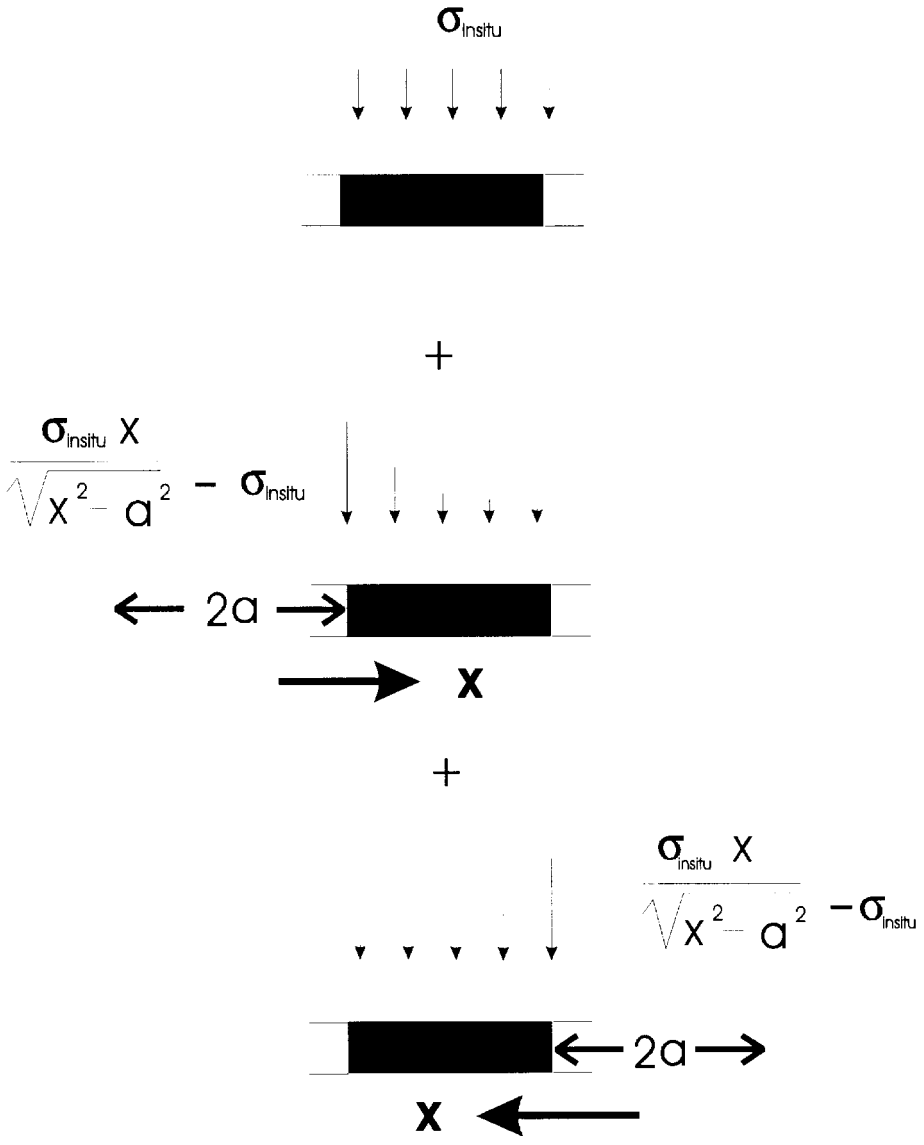

Figure 23.—Pillar stress broken down into three components.

The left stress component has the origin of its axis located to the left of the pillar. The positive direction, relative to this axis, is rightward from the origin into the pillar. The right component is the mirror image of the left. This component has the origin of its axis to the right of the pillar. The variable "a" can have a different value for each side of the pillar (figure 23). The total stress distribution on the pillar is equal to the left component plus the uniform in situ stress plus the right component. As verified by FLAC, the superposition technique accurately predicts the stress distribution across a single pillar (figure 24).

A mine opening affects the stress distribution for a substantial distance. A mine panel consists of a gridwork of entries and crosscuts. It is necessary to superimpose the stress components from all mine passageways. FLAC compares the results of the superposition across an entire mine panel (figure 25).

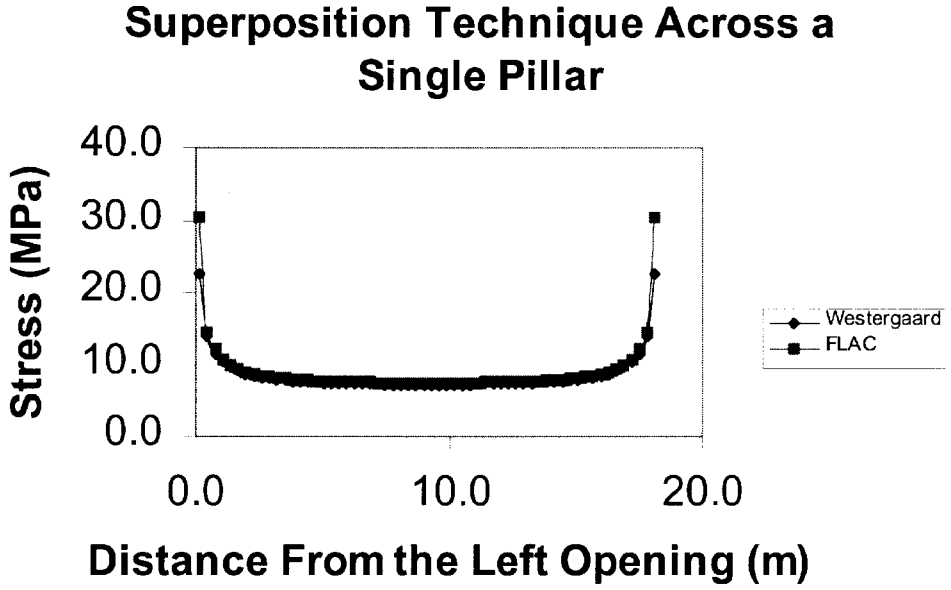

Figure 24.—Pillar with stress superimposed from both sides.

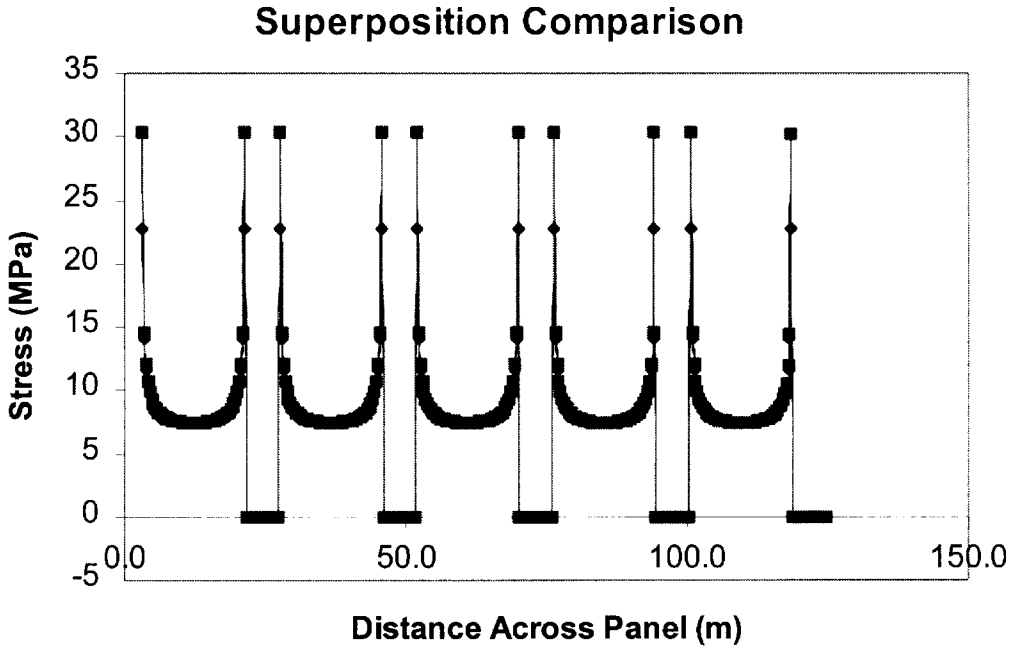

Figure 25.—Westergaard equation and superpositioning stress over an entire mine panel. Comparison with numerical model.

POSSIBLE ENHANCEMENTS

It is possible to enhance the modeling capabilities of the FMA. Adding other techniques would give the ability to analyze displacements in the strata, creep behavior in mine supports, and the effects of multiple-seam mining. Because the FMA is straightforward and easy to use, there is potential to model many different mining situations.

The following sections discuss some possible additions to the FMA. Although each technique presented seems reasonable, no comparison has been made with numerical analysis to qualify accuracy.

VIEW OF STRESS DISTRIBUTION FROM A PLANAR PERSPECTIVE

Sometimes it is desirable to study the stress distribution looking down on the coal seam (planar view) instead of into it (cross-sectional view). In a planar view, coal pillars are rectangular. The corners of the pillar generate mathematical singularities that create problems for analysis. One way to eliminate the singularities is to assume the pillar is an ovaloid instead of a rectangle [Kramer 1996]. It is possible to segment the pillar into concentric ovaloid lines of equal distance (figure 26). Fracture mechanics predicts the stress distribution through the pillar centers, as indicated by the vertical and horizontal lines in figure 26. An interpolation technique can approximate the stress throughout the pillar by using the concentric ovaloid arcs as interpolation pathways. For instance, the arc segment between points A and B in figure 26 would be the interpolation path between the stresses at points A and B. It is easy to interpolate the stresses along ovaloid paths. The basic equations for mapping elliptical coordinates to Cartesian coordinates are:

$$x = a \cos 2 \qquad y = b \sin 2 \qquad (23)$$

An example of the interpolation process follows.

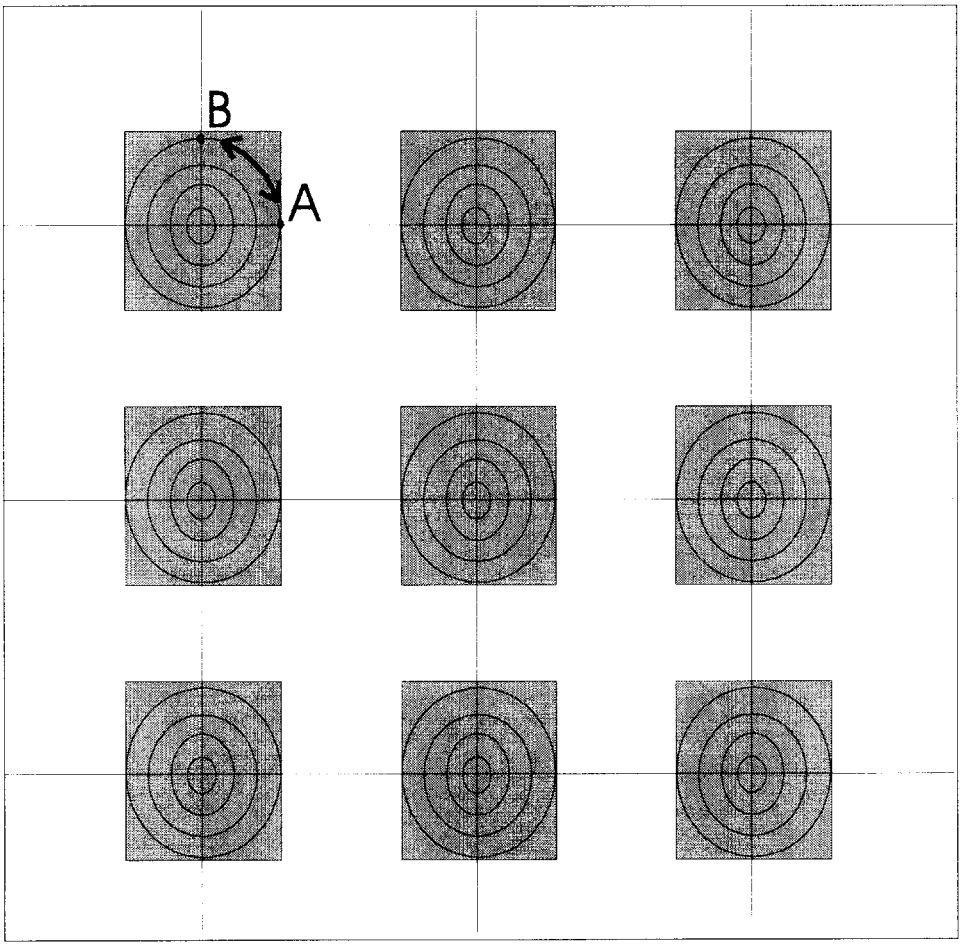

Figure 26.—Fracture mechanics predicts the center stress in both directions through the pillar. An interpolation technique translates the stress along the elliptical trajectories.

EXAMPLE OF INTERPOLATION

Considering the elliptical path shown in quadrant I of figure 27, interpolate the stresses along path A-B in the outer arc of quadrant I. For this example, assign the following properties:

$F_A = 1{,}000$ psi

$F_B = 1{,}500$ psi

$a = 20$

$b = 10$

Divide 2 into five equal angles:

$$\frac{90}{5} = 18° \tag{24}$$

Determine the stress interpolation interval for each 18° arc:

$$\frac{1{,}500 \text{ psi} - 1{,}000 \text{ psi}}{5 \text{ intervals}} = 100 \text{ psi per interval} \tag{25}$$

Figure 28 illustrates the stress distribution along this arc. Equation 24 relates any point on the A and B axis to any point on the ovaloid (figure 27). Therefore, it is possible to approximate the stress distribution throughout the entire pillar.

VISCOELASTICITY

Sih [1966] and Paris and Sih [1965] discuss crack behavior in viscoelastic (time-dependent) material. For viscoelastic material, the crack-tip stress field is the same, only the stress intensity factors K_I are functions of time, such that

$$K_I = K_I(t) \tag{26}$$

This function shows promise for future applications using the FMA. For instance, it could be valuable for studying the behavior of salt.

DISPLACEMENTS

Fracture mechanics may also predict the displacement/strain in a mine environment. A common method to predict displacement is referred to as the "crack opening displacement" (COD) [Broek 1982]. The COD method takes into account the total displacement of the crack surface (figure 29). In mining, the COD predicts the combined displacement of the roof and floor of an opening, such that

$$\text{COD} = 2v = \frac{4F}{E}\sqrt{a^2 - x^2} \tag{27}$$

and at the center of the opening:

$$\text{COD}_{max} = 2v = \frac{4Fa}{E}. \tag{28}$$

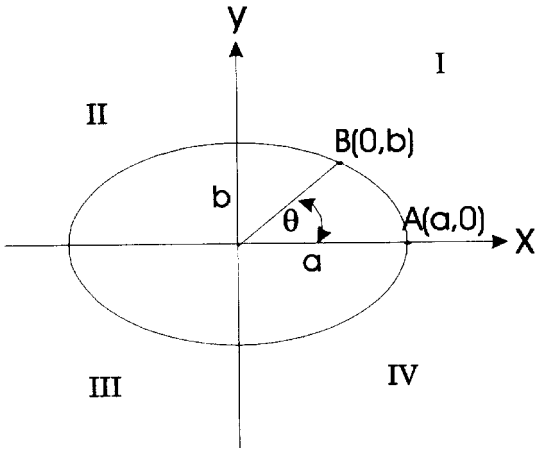

Figure 27.—Relationship between elliptical and rectilinear coordinates.

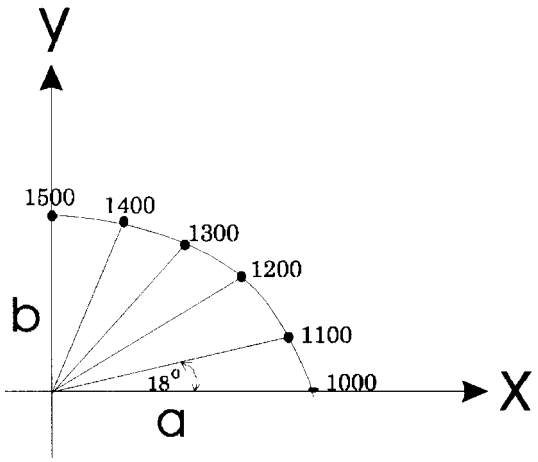

Figure 28.—Stresses distributed along interpolation arc.

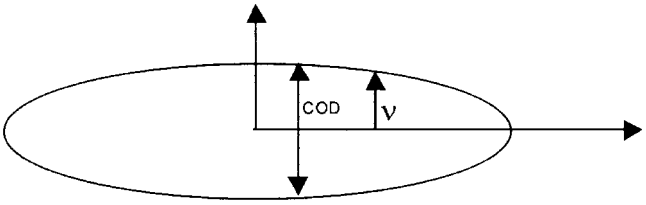

Figure 29.—The crack opening displacement (COD) method considers the displacement of the entire surface of a crack.

MULTIPLE-SEAM MINING

It may be possible to predict the effects on stress distribution caused by mining activity in seams above or below the area of interest. By using stress influence functions developed for mine subsidence prediction, it should be possible to predict multiple-seam influences with a respectable degree of accuracy [Luo 1997]. This multiple-seam model could be more accurate than other numerical methods because most other methods use influence functions based on the theory of elasticity, which assumes infinitesimal displacements. Using influence functions based on mine subsidence profiles takes into account the well-documented, large-scale displacements measured at various mine locations.

CONCLUSION

This paper presents the FMA for predicting the stresses in a mine panel. It can model any combination of mine supports such as longwall gob, yield pillars, cribs, chocks, posts, automated temporary roof supports, and hydrostatic loads. The technique uses an analytic expression; thus, it is fast, simple, and accurate. It simulates pillar yield by combining the analytic equation with any empirical pillar strength equations. The procedure incorporates easily into spreadsheets or computer software. The FMA predicts pillar stress with a high degree of accuracy; however, it is no match to good numerical modeling software. Its main function is to be quick and simple in order to encourage nonspecialized personnel to use it as a guide for studying mine supports.

The FMA works well for coal seams aligned along a horizontal plane. Additional effort is needed to assess its accuracy for seams aligning along inclined planes. More work is also necessary to develop FMA techniques for thick-seam mining, multiple-seam mining, and displacement prediction. Computer software featuring the FMA is available from the author.

REFERENCES

Barenblatt G [1962]. The mathematical theory of equilibrium of cracks in brittle fracture. Advances in Appl Mech *7*:55-129.

Berry D [1960]. An elastic treatment of ground movement due to mining isotropic ground. J Mech Phys Solids *8*:280-292.

Berry D [1963]. Ground movement considered as an elastic phenomenon. Trans Inst Min Eng *123*:28-41.

Broek D [1982]. Elementary engineering fracture mechanics. 3rd ed. The Hague, The Netherlands: Martinus Mijhoff Publishers.

Crouch SL, Fairhurst C [1973]. The mechanics of coal mine bumps and the interaction between coal pillars, mine roof, and floor. U.S. Department of the Interior, Bureau of Mines, OFR 53-73.

Dugdale D [1960]. Yielding of steel sheets containing slits. J Mech Phys *8*:100-108.

Hacket P [1959]. Analytic analysis of rock movements caused by mining. Trans Inst Min Eng *118*(7):421-433.

Karabin GJ, Evanto MA [1999]. Experience with the boundary-element method of numerical modeling to resolve complex ground control problems. In: Proceedings of the Second International Workshop on Coal Pillar Mechanics and Design. Pittsburgh, PA: U.S. Department of Health and Human Services, Public Health Service, Centers for Disease Control and Prevention, National Institute for Occupational Safety and Health, DHHS (NIOSH) Publication No. 99-114, IC 9448.

Kramer JM [1996]. The use of fracture mechanics to predict the stress distribution in coal mine pillars [Dissertation]. Morgantown, WV: West Virginia University, Department of Mining Engineering.

Kramer JM, Luo Y, Peng SS [1998]. An analytic approach to determine the stress distribution in longwall chain pillars. In: Peng SS, ed. Proceedings of the 17th International Conference on Ground Control in Mining. Morgantown, WV: University of West Virginia, pp. 162-168.

Luo Y [1997]. Private conversation between J. Kramer, Mine Safety and Health Administration, and Y. Luo, West Virginia University, Morgantown, WV.

Mark C, Iannacchione AT [1992]. Coal pillar mechanics: theoretical models and field measurements compared. In: Proceedings of the Workshop on Coal Pillar Mechanics and Design. Pittsburgh, PA: U.S. Department of the Interior, Bureau of Mines, IC 9315, pp. 78-93.

Paris P, Sih G [1965]. Stress analysis of cracks. ASTM STP *391*: 30-81.

Salamon MDG, Munro AH [1967]. A study of the strength of coal pillars. J S Afr Inst Min Metall *68*:55-67.

Sih G [1966]. On the Westergaard method of crack analysis. Inter J Fracture Mech *2*:628-631.

Westergaard H [1939]. Bearing pressures and cracks. ASME J of Appl Mech *61*:A49-53.

Wilson AH [1972]. An hypothesis concerning pillar stability. Min Eng (London) *131*(141):409-417.